Learning in Chaos: Efficient Autoscaling and Self-healing for Distributed Training at the Edge

Wenjiao Feng, Rongxing Xiao, Zonghang Li[†], Hongfang Yu, Gang Sun, Long Luo, Mohsen Guizani, *Fellow, IEEE*, and Qirong Ho

Abstract—Frequent node and link changes in edge AI clusters disrupt distributed training, while traditional checkpoint-based recovery and cloud-centric autoscaling are too slow for scaleout and ill-suited to chaotic and self-governed edge. This paper proposes Chaos, a resilient and scalable edge distributed training system with built-in self-healing and autoscaling. It speeds up scale-out by using multi-neighbor replication with fast shard scheduling, allowing a new node to pull the latest training state from nearby neighbors in parallel while balancing the traffic load between them. It also uses a cluster monitor to track resource and topology changes to assist scheduler decisions, and handles scaling events through peer negotiation protocols, enabling fully self-governed autoscaling without a central admin. Extensive experiments show that Chaos consistently achieves much lower scale-out delays than Pollux, EDL, and Autoscaling, and handles scale-in, connect-link, and disconnect-link events within 1 millisecond, making it smoother to handle node joins, exits, and failures. It also delivers the lowest idle time, showing superior resource use and scalability as the cluster grows.

Index Terms—Distributed machine learning, autoscaling, self-healing, elastic training.

I. INTRODUCTION

The rapid growth of model and cluster sizes is pushing AI training to its limits. At OpenAI, a hidden bug caused frequent crashes during GPT-4.5 training, forcing constant checkpointing and restarts [1]. DeepSeek [2] reallocates inference machines for model training at night, requiring clusters to scale up and down on the fly. The demand for self-healing and autoscaling is even more urgent in edge AI training, where devices are more unstable and free to join and leave.

(a) Edge devices and their interconnections are more prone to interruptions. They are decentralized and unpredictable, they can drop out at any time due to failures in network, device and software, and power loss, movement, user

This work was supported in part by National Natural Science Foundation of China (62394324) and Young Elite Scientists Sponsorship Program by CAST (2022QNRC001).

W. Feng, R. Xiao, H. Yu, G. Sun, and L. Luo are with the School of Information and Communication Engineering, University of Electronic Science and Technology of China (UESTC), Chengdu, 611731, China (email: fwj0612, yzzxrx}@gmail.com, fyuhf, gangsun, llong}@uestc.edu.cn).

Z. Li, M. Guizani, and Q. Ho are with the Department of Machine Learning, Mohamed bin Zayed University of Artificial Intelligence (MBZUAI), Building 1B, Masdar City, Abu Dhabi, United Arab Emirates (email: {zonghang.li, mohsen.guizani, Qirong.Ho}@mbzuai.ac.ae).

Corresponding authors are Z. Li and H. Yu.

- interrupts. Even if devices remain alive, unstable connections caused by routing failures, firewalls, congestion, or mobility can still disrupt training.
- (b) Edge devices are self-governed and free to join, leave, and switch networks at will. They may join when idle or charging, and leave under heavy load or to save RAM/CPU/energy. They are also free to join or leave a network, leading to new or terminated connections.

Changes in cluster nodes and links can interrupt distributed training. A common fix to handle unexpected node dropouts is checkpointing and restart: save model checkpoints, fix the issue, then roll back and restart training from checkpoints [1], [3]–[7]. This stop-resume method also applies to autoscaling: stop training when nodes join or leave, reinit the cluster, and restart training from the last checkpoint [8]–[12]. This process is time- and resource-costly due to heavy disk I/O from frequent checkpointing. To address this, stop-free autoscaling [13]–[17] lets new nodes pull the latest training state from running nodes, no restarts, and no checkpoints. This enables continuous and scalable training at chaotic edge.

While these systems have supported self-healing or autoscaling, they are slow in practice. When a new node joins, it must pull the latest training state, such as model weights and optimizer state, from a running node. This time cost is called state replication delay. In data centers, fast and symmetric LANs keep this delay low, even when pulling from a random node [8]–[11], [13]–[17]. At the edge, however, limited bandwidth can stretch delays to tens of seconds, or even minutes if the pulling node is far away in an asymmetric, uneven network. Such high delays are unacceptable for fast-changing edge clusters. To keep training smooth, replication must be optimized for fast act to node and link changes.

Secondly, existing systems are designed for the HPC, not the edge. They support either self-healing or autoscaling, but edge clusters demand both because the network environment is far more chaotic. In addition, current autoscaling is centrally managed, i.e., there is an admin monitoring cluster load and manually triggering scaling up/down. In contrast, edge devices are decentralized and self-governed, with no central control. As a result, edge training systems must react on their own, detecting node and link changes and fixing communication rules at runtime with no admin involved.

This paper proposes Chaos, a resilient and scalable edge distributed training system with self-healing and autoscaling.

Chaos monitors cluster and resource changes in real time. When nodes or links join, leave, or fail, it automatically triggers scale-in, scale-out, connect-link, and disconnect-link actions. It removes faulty nodes or links, resolves cluster blocking, scales the cluster up or down, and fixes communication rules on the fly. To speed up state replication for new nodes, we introduce a neighbor-aware mechanism. It uses the overlay network topology and resources detected by Chaos to find neighbor nodes, and pulls the training state from them in parallel, using multi-path transfer and traffic scheduling for faster replication. We set up an edge cluster with 6-12 virtual machines, simulating node joins and exits under constrained, heterogeneous network conditions. The results show that, compared to alternatives in Pollux [8], EDL [13], and Autoscaling [18], our Chaos handles self-healing and autoscaling more efficiently.

Our main contributions are summarized as follows:

- We propose a resilient, scalable edge distributed training system with self-healing and autoscaling that can more efficiently handles node and link joins, exits, and failures.
- We propose a multi-neighbor state replication mechanism that pulls the training state from neighbors in parallel, with a shard scheduler to balance their traffic load.
- We propose a cluster monitor that tracks resource and topology changes, along with peer negotiation protocols that enable autoscaling without a central admin.
- We implement Chaos and show that it achieves much lower scale-out delays than Pollux, EDL, and Autoscaling, with superior resource efficiency and scalability.

II. RELATED WORK AND MOTIVATIONS

A. Reviews on Self-healing and Autoscaling

Self-healing. In distributed machine learning (DML), worker nodes frequently synchronize model weights, but in edge networks, frequent node and link failures block synchronization and freeze training. Checkpointing helps recover from such failures by periodically saving the training state, e.g., model weights, optimizer states, so the system can restart from the last checkpoint [1], [7]. DataStates-LLM [3] and CheckFreq [19] reduce training stalls by asynchronously writing checkpoints. JIT [4] triggers checkpointing on other nodes only after a failure occurs. Check-N-Run [5] uses differential storage to cut checkpoint size. Gemini [20] speed up recovery by redundantly storing checkpoints in RAM across devices.

Autoscaling. Checkpointing is also a key approach to autoscaling, known as the "stop-resume" strategy [13]. It saves a checkpoint, pauses training, resizes the cluster, then restarts training from the latest checkpoint. To reduce the checkpointing overhead, Optimus [9] triggers autoscaling detection every ten minutes. Pollux [8] saves checkpoints only when cluster size and topology need to change. Rubick [12] sets an empirical threshold and only reconfigures when restart overhead stays below it.

Stop-free autoscaling offers a faster and more flexible alternative. When a new node joins, it pulls the training state

directly from active nodes' memory, so no need to restart training or load/write checkpoints from/to a slow disk. In parameter server setups [21], PaddleEDL [22] and ElasticDL [23] use asynchronous training to realize stop-free autoscaling. As workers run independently, their join and exit don't disrupt others, and new nodes can simply fetch the latest model from the parameter server. However, they fall back to stop-resume in synchronous mode. DL2 [11] enables stop-free autoscaling in synchronous training using a scaling clock that detects new nodes and sends them the current model. In more general cases, systems like EDL [13], EPS [15], CoDDL [16], and DeepBoot [17] typically select a node (e.g., master) to pull the training state from. Elan [14] instead picks the neighbor with the highest bandwidth. Autoscaling [18] takes it further by slicing the training state across multiple nodes and pulling from them in parallel for faster replication.

A key limitation of these systems is that they are designed for centralized HPC clusters, not for the decentralized and autonomous edge. For example, Autoscaling adds nodes every few minibatches. EDL, EPS, Elan, CoDDL, and DeepBoot scale based on cluster load. DeepSeek offloads inference nodes to training clusters during idle hours. Pollux and Rubick schedule GPU resources and decide when and how much to scale. In these systems, a central admin makes the scaling decisions, and scaling happens in batches. However, the join and leave models at the edge are fundamentally different:

- Chaos doesn't need GPU scheduling like others do. User devices are free to join or leave at any time. Even if the admin could make optimal scheduling decisions, it cannot command users to join, as users may not cooperate.
- Users' joins and leaves follow a Poisson process, arriving one by one. This process follows the laws of nature, making GPU scheduling useless. Chaos must handle user joins and leaves one by one, unlike HPC schedulers that plan for batched changes.

Since user joins and leaves must be handled one by one, what matters more is how to make scaling fast, as scale-in and scale-out happen far more frequently than a batched change. This calls for a new, edge-native solution.

B. Motivations

Question A: Which node(s) should a new node pull from for faster state replication?

Most systems let a new node pull the training state from a single node [13]–[17]. In the case shown in Figs. 1a and 1b, a new node 11 joins and picks the fastest neighbor to pull from, but sending the entire state over a single link creates a bottleneck, replication still takes 80 time units. Autoscaling [18] provides a multi-source solution by splitting the training state and pulling shards from multiple nodes in parallel. While effective in symmetric networks like fat-trees, it performs poorly in irregular edge networks, e.g., in Fig. 1c, where distant nodes require multi-hop forwards, causing delays of up to 88 time units, even along the shortest routes.

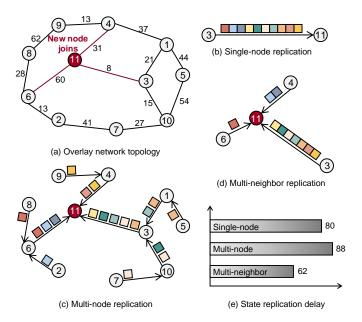


Fig. 1: An example of (a) the overlay network topology, (b) single-node replication, (c) multi-node replication, and (d) multi-neighbor replication. (e) compares their state replication delays. The number on each edge indicates the delay incurred to transfer one unit of data through that link. Suppose there are 10 data units to transmit.

It is clear that multi-hop forwards involves significant redundant transfers. In synchronous training, all nodes share the same model weights, so paths like $7 \rightarrow 10 \rightarrow 3 \rightarrow 11$ are wasteful, node 3 already has the data shards of nodes 7 and 10. Instead, node 3 alone can serve node 11, cutting unnecessary hops and transmission. This inspires *multi-neighbor replication*, where the new node pulls shards directly from its neighbors, as shown in Fig. 1d. With smart shard sizing, replication delay drops to 62 time units. This calls for *a shard scheduler that minimizes the completion time to pull from all neighbors*.

Question B: How does a new node join a decentralized, self-governed edge cluster?

Existing systems [13]–[18] rely on an admin to manually trigger autoscaling. As shown in Fig. 2a, the new node keeps waiting until the admin decides to scale out and sends a command to initialize and join the cluster. This, however, does not work in a decentralized, self-governed edge cluster. There is no central admin to send such commands. Without it, new nodes are left waiting indefinitely. This motivates a shift: instead of waiting for a command that will never come, new nodes should take the initiative and actively send join requests. As shown in Fig. 2b, the new node actively connects to the cluster scheduler and runs stop-free autoscaling through self-discovery, peer negotiation, and state synchronization. Therefore, we need a cluster monitor to detect node and link changes, and peer-negotiation protocols for flexible scale-in, scale-out, connect-link, and disconnect-link events.

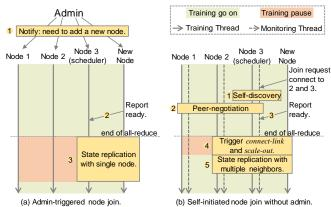


Fig. 2: Illustration of node joins with and without an admin.

To address question A, Section III mathematically models the shard assignment problem, introduces a polynomial-time algorithm, and analyzes its optimality gap and complexity. Then, for question B, Section IV presents the cluster monitor and peer negotiation protocols for scale-out, scale-in, connect-link, and disconnect-link. Section V outlines the overall system design, and Section VI provides the experiment results.

III. MULTI-NEIGHBOR STATE REPLICATION

When a new node joins, it needs to pull training states from existing nodes, including model weights, optimizer states, and runtime info like epoch, iteration, hyperparameters, and so on. These states are consistent across nodes because the training is synchronous. As shown in Fig. 3, model weights and optimizer states take up most of the size. Even pulling from a neighbor can take up to one minute, which is far too slow for an edge cluster with frequent node joins. To speed things up, this section models a shard assignment problem based on multineighbor replication, and propose a fast algorithm to cut the scale-out delay.

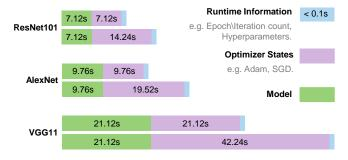


Fig. 3: Overview of replication delays for each component. The link bandwidth is set to 200 Mbps.

A. Problem Model

Let G=(V,E) be a graph shown in Fig. 1a, with each edge has a weight representing the delay of transmitting one

unit of data over that link. Given a DML task with training state w (e.g., model weights and optimizer states). For a finegrained control over traffic load, we split w into K shards, each with data size s. Assume s can divide the total data size |w|, that is, |w| = Ks. Let $\mathcal{K} = \{w_1, w_2, \cdots, w_K\}$ be the set of model shards. Now, a new node v_{new} joins and needs to pull shards $\mathcal{K} = \{\mathcal{K}_1, \cdots, \mathcal{K}_{|\mathcal{U}|}\}$ from its neighbors \mathcal{U} , where each neighbor $u \in \mathcal{U}$ provides a shard subset $\mathcal{K}_u \subset \mathcal{K}$. These shard subsets are disjoint and their collection covers all shards, i.e., $\bigcup_{u\in\mathcal{U}}\mathcal{K}_u=\mathcal{K} \text{ and } \mathcal{K}_u\cap\mathcal{K}_v=\emptyset \text{ for any } u\neq v.$

Let $t_{u o v_{
m new}}^{
m prop}$ be the propagation delay and $t_{u o v_{
m new}}^{
m trans}$ the perparameter transmission delay from neighbor u to v_{new} . Then, the delay to send all shards in the set \mathcal{K}_u is:

$$t_u(s, \mathcal{K}_u) = t_{u \to v_{\text{new}}}^{\text{prop}} + s \cdot t_{u \to v_{\text{new}}}^{\text{trans}} \cdot |\mathcal{K}_u|. \tag{1}$$

As shown in Fig. 2b, state replication starts after the allreduce, but neighbors finish all-reduce at different times. Let au_u^{sync} be the time when neighbor u finishes all-reduce. Our goal is to minimize the latest completion time any neighbor finishes its replication:

$$\min_{s,\mathcal{K}_u} \max_{u \in \mathcal{U}} \quad t_u(s,\mathcal{K}_u) + \tau_u^{\text{sync}},$$
s.t. $s \in \mathbb{Z}^+, |\mathcal{K}_u| > 0, \forall u \in \mathcal{U}.$ (3)

s.t.
$$s \in \mathbb{Z}^+, |\mathcal{K}_u| > 0, \forall u \in \mathcal{U}.$$
 (3)

To formally represent K_u , we introduce a binary selection matrix $x_{uj} \in \{0,1\}$, where $u \in \mathcal{U}$ is a neighbor of the new node and $j \in \{1, 2, \dots, K\}$ indexes the model shards. If $x_{uj} = 1$, neighbor u sends shard w_i ; otherwise, it doesn't. Thus, the problem can be reformulated as **P1**:

$$\min_{s, x_{uj}} \max_{u \in \mathcal{U}} \quad t_u(s, x_{uj}) + \tau_u^{\text{sync}}, \tag{4}$$

s.t.
$$t_u(s, x_{uj}) = t_{u \to v_{\text{new}}}^{\text{prop}} + \sum_{i=1}^{K} s \cdot t_{u \to v_{\text{new}}}^{\text{trans}} \cdot x_{uj},$$
 (5)

$$\sum_{u \in \mathcal{U}} x_{uj} = 1, \ \forall j \in \{1, 2, \cdots, K\},\tag{6}$$

$$s \in \mathbb{Z}^+, |\mathcal{K}_u| > 0 \ \forall u \in \mathcal{U}.$$
 (7)

This objective involves a max operation, so we introduce an auxiliary variable θ to bound the completion time across all neighbors. Then the problem becomes **P2**:

$$\min_{\mathbf{s}, x_{v,i}, \theta} \quad \theta \tag{8}$$

s.t.
$$t_u(s, x_{u,i}) + \tau_u^{\text{sync}} \le \theta, \ \forall u \in \mathcal{U},$$
 (9)

$$t_u(s, x_{uj}) = t_{u \to v_{\text{new}}}^{\text{prop}} + \sum_{j=1}^{K} s \cdot t_{u \to v_{\text{new}}}^{\text{trans}} \cdot x_{uj}, \quad (10)$$

$$\sum_{i=1}^{n} x_{ij} = 1, \ \forall j \in \{1, 2, \cdots, K\},$$
 (11)

$$s \in \mathbb{Z}^+, x_{uj} \in \{0, 1\} \ \forall u, j.$$
 (12)

The constraint includes a product of variables, $s \cdot x_{uj}$, where s is an integer and x_{uj} is binary. This makes the problem a mixed integer nonlinear programming (MINLP) and hard to solve. To make it easier, we hope to fix s in P2 so that it becomes a linear program.

If we fix x_{ui} and optimize only s, the problem P2 becomes:

$$\min_{s} \max_{u \in \mathcal{U}} \alpha_u \cdot s + \beta_u, \text{ s.t. } s \in \mathbb{Z}^+, \tag{13}$$

where $\alpha_u > 0, \beta_u > 0$ are constants. Since the objective is a max over linear functions, the overall objective is monotonically increasing with respect to s. Although θ in P2 is not strictly monotonic, it often exhibits a quasi-monotonic trend in practice, making binary search an effective way to quickly find a near-optimal s, as described in Algorithm 1.

Then, we can apply an external binary search to fix s and focus on optimizing x_{uj} . The problem P2 now becomes P3:

$$\min_{x_{ni},\theta} \quad \theta \tag{14}$$

s.t.
$$t_u(x_{uj}) + \tau_u^{\text{sync}} \le \theta, \ \forall u \in \mathcal{U},$$
 (15)

$$t_u(x_{uj}) = t_{u \to v_{\text{new}}}^{\text{prop}} + s \cdot t_{u \to v_{\text{new}}}^{\text{trans}} \cdot \sum_{j=1}^{K} x_{uj}, \quad (16)$$

$$\sum_{u \in \mathcal{U}} x_{uj} = 1, \ \forall j \in \{1, 2, \cdots, K\},\tag{17}$$

$$x_{uj} \in \{0, 1\}, \ \forall u, j.$$
 (18)

P3 is a mixed integer linear programming (MILP) with binary variables. It is more tractable to solve than a MINLP in P2, with standard MILP solvers. By iterating over possible values of s using binary search, we can efficiently find the optimal shard assignment \mathcal{K}_u^* , $\forall u \in \mathcal{U}$.

However, even as a standard MILP, P3 remains NP-hard. With large models and complex networks, solving P3 can take several seconds. Since P2 uses binary search over s, P3 must be solved multiple times, pushing the total delay into tens of seconds. This solution delay even exceeds the state replication time, making the MILP solver impractical. Worse, every new node triggers a fresh solve, further tightening the latency constraints. To keep things fast, we trade the mathematically elegant but slow MILP solver for a **fast greedy** algorithm (Algorithm 2). This greedy solution provides a bounded optimality gap and can find a near-optimal solution in a flash, making it more well-suited for practical use.

B. Algorithm Design

The training state w contains many tensors of varying sizes, small ones like convolution kernels and biases, and large ones like fully connected layer weights. Assigning these raw tensors directly to neighbors creates uneven traffic loads, causing the coflow completion time to spike. To better balance traffic, we introduce s in P2 to control the model shard size after splitting. If s is set too large, shards are few and traffic stays uneven; but if it is set small, transmission becomes inefficient. Leveraging the quasi-monotonic nature of P2 with respect to s, Algorithm 1 uses binary search to quickly find a good value. In each iteration, it splits the training state w into shards $\mathcal{K} = \{w_1, w_2, \cdots, w_K\}$ of size s, then calls the P3

Algorithm 1: Shard Assignment with Binary Search (P2)

```
Input: Training states w, neighbor set \mathcal{U}, new node v_{\text{new}}.
    Output: Shard assignment \{\mathcal{K}_u^*, \forall u \in \mathcal{U}\}, Shard size s^*
 1 Initialize s_l \leftarrow \min_{\text{layer\_size}}(w), s_h \leftarrow \max_{\text{layer\_size}}(w);
2 Initialize the objective value \theta^* \leftarrow +\infty;
3 while s_l \leq s_h do
           Set s \leftarrow \lfloor \frac{s_l + s_h}{2} \rfloor;
 4
           Split tensors in w into a set of shards K, each of size s;
 5
 6
           Solve P3 with given K and s:
           \{\mathcal{K}_u, \forall u\} \leftarrow \mathsf{Greedy} \; \mathsf{Shard} \; \mathsf{Assignment}(\mathcal{K}, \mathcal{U}, s, v_{\mathsf{new}});
 7
           Calculate objective value \theta in P2 with given \mathcal{K}_u and s;
 8
           if \theta < \theta^* then
 9
                  \theta^* \leftarrow \theta, \, \mathcal{K}_u^* \leftarrow \mathcal{K}_u, \, s^* \leftarrow s,
10
                 s_h \leftarrow s - 1;
11
12
                 s_l \leftarrow s+1;
13
14 return \{\mathcal{K}_u^*, \ \forall u \in \mathcal{U}\}, s^*;
```

Algorithm 2: Greedy Shard Assignment (P3)

```
Input: Model shard set \mathcal{K}, neighbor set \mathcal{U}, shard size s, new node v_{\text{new}}, propagation delay t_{u \to v_{\text{new}}}^{\text{prop}}, transmission delay t_{u \to v_{\text{new}}}^{\text{prop}}, synchronization delay \tau_u^{\text{sync}} for each u \in \mathcal{U},

Output: Shard assignment \{\mathcal{K}_u\} for each u \in \mathcal{U}.

1 Initialize the assignment \mathcal{K}_u \leftarrow \emptyset, \forall u \in \mathcal{U};

2 Initialize the load l_u = t_{u \to v_{\text{new}}}^{\text{prop}} + \tau_u^{\text{sync}}, \forall u \in \mathcal{U};

3 foreach shard w_k \in \mathcal{K} of size s do

4 Select the neighbor u^* with least estimated load: u^* \leftarrow \arg\min_u(l_u + s \cdot t_{u \to v_{\text{new}}}^{\text{trans}});

5 Assign the shard w_k to neighbor u^*: \mathcal{K}_{u^*} \leftarrow \mathcal{K}_{u^*} \cup \{w_k\};

6 Update the load: l_{u^*} \leftarrow l_{u^*} + s \cdot t_{u^* \to v_{\text{new}}}^{\text{trans}};

7 return \{\mathcal{K}_u, \ \forall u \in \mathcal{U}\};
```

solver (Algorithm 2) to assign shards to neighbors. If the result improves, binary search continues on a smaller size; otherwise, it tries a larger size. This search repeats until the optimal shard size s^* and assignment $\{\mathcal{K}_u^*, \ \forall u \in \mathcal{U}\}$ are found.

To solve P3, Algorithm 2 takes a greedy approach: it iteratively assigns shards to the neighbor with the lowest estimated load. To see how the estimate load l_u is updated, we rewrite P3 as the following min-max problem:

$$\min_{x_{uj}} \max_{u \in \mathcal{U}} \quad \underbrace{t_{u \to v_{\text{new}}}^{\text{prop}} + \tau_{u}^{\text{sync}}}_{\text{initial term}} + \sum_{j=1}^{K} \underbrace{s \cdot t_{u \to v_{\text{new}}}^{\text{trans}}}_{\text{update term}} \cdot x_{uj} \tag{19}$$

Following this pattern, we initialize l_u using the fixed term (the initial term), $t_{u \to v_{\rm new}}^{\rm prop} + \tau_u^{\rm sync}$, and increment it with the per-shard cost (the update term), $s \cdot t_{u \to v_{\rm new}}^{\rm trans}$. The initial term captures the base delay before neighbor u can start transmitting a shard, and the update term captures the delay for transmitting one shard to the new node. Then, it looks at all neighbors, picks the neighbor u^* with the lowest estimate load, assigns the shard to u^* , and updates its load l_{u^*} accordingly.

Optimality Gap. This greedy solution tries to equalize the delay by always choosing the least-loaded neighbor. It

reduces to the longest processing time first (LPT) heuristic for the $P\|C_{\max}$ scheduling problem. By Graham's bound [24], LPT achieves a makespan no worse than $(\frac{4}{3}-\frac{1}{3|\mathcal{U}|})\cdot \text{OPT}$, where OPT is the optimal value. That means Algorithm 2 is guaranteed to stay within 33% of the optimum, and in typical cases where neighbors are few (e.g., $|\mathcal{U}|=2$), the optimality gap improves to just 17%.

Complexity Analysis. Algorithm 1 performs a binary search over the shard size s, with at most $O(\log S)$ steps, where S is the range of shard sizes. In each step, it runs Algorithm 2 to assign K shards to $|\mathcal{U}|$ neighbors, taking $O(K \cdot |\mathcal{U}|)$ per step. Thus, the total time complexity of Algorithm 1 is $O(K \cdot |\mathcal{U}| \cdot \log S)$, which is in polynomial time.

To sum up, our algorithms come very close to optimal and run orders of magnitude faster than solving the MINLP/MILP, which is further validated in our experiments.

IV. CLUSTER MONITOR AND PEER NEGOTIATION

In the previous section, we showed how shard scheduling can speed up state replication when new nodes join, but two issues remain:

- 1) The algorithms rely on prior knowledge of the cluster topology and resources, like which nodes are neighbors, and the link latency and bandwidth between them.
- The algorithms are triggered by cluster changes, such as node joins, exits, and failures, so they rely on timely detection of these events to respond to changes.

In this section, we first introduce a cluster monitor to track resources for scheduling decisions and to detect node and link changes, followed by peer-negotiation protocols to handle scale-in/out and connect/disconnect-link events.

A. Cluster Monitor

As stated above, the cluster monitor plays three key roles: tracking the cluster topology, detecting node and link changes, and monitoring network resources.

Cluster Topology Monitoring. The primary task of the cluster monitor is to detect the overlay topology. In Chaos, this is handled by the scheduler, which tracks each node's ID, state (e.g., active, failed, or standby), neighbors, and join time. This data helps scheduling algorithms (e.g., Algorithms 1 and 2) identify neighbors \mathcal{U} and quickly spot changes to trigger scaling events. It also supports DML systems like NetStorm [25] to build their all-reduce strategies.

Cluster Event Monitoring. In Chaos, scaling events are triggered by node and link changes. The cluster monitor listens for control messages to detect joins and exits, and uses heartbeat and probe messages to identify failures:

- *Node joins:* When a new node joins, it sends a *scale-out* message to the scheduler with its IP-port and available links, then Algorithms 1 and 2 are invoked.
- Node exits: When a node leaves, it sends a scale-in message to the scheduler.

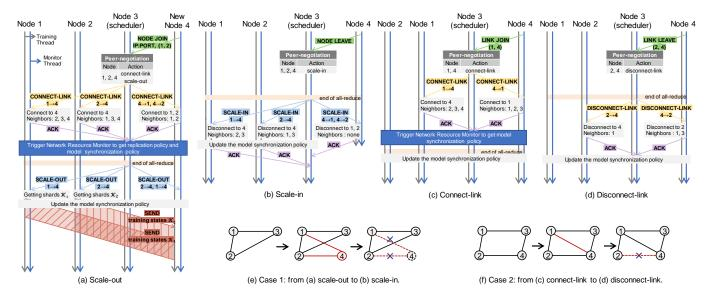


Fig. 4: Peer negotiation protocols for scale-out, scale-in, connect-link, and disconnect-link.

TABLE I: Summary of scaling primitives in Chaos

Primitives	Functionality	Event	Delay
Scale-out	Add a node, connect it to neighbors, and synchronize training state.	Node joins	0.5-5 s
Scale-in	Remove a node and terminate its sockets to neighbors.	Node exits or failure	<1 ms
Connect-link	Establish a new socket between two nodes.	Link joins	<1 ms
Disconnect-link	Terminate the socket between two nodes.	Link exits or failure	<1 ms

- Node failure: Chaos uses heartbeats to track liveness.
 Each node sends a heartbeat to the scheduler every few seconds. If no heartbeat arrives within a set time, the node is considered lost, and scale-in is triggered.
- *Link joins:* To create a new link, a node sends a *connect-link* message to the scheduler, specifying the target node.
- *Link exits:* To remove a link, a node sends a *disconnect-link* message to the scheduler, specifying the target node.
- Link failure: Link failures are detected using probes. If two nodes fail to measure bandwidth or latency on a link, it is considered down, and one end sends a disconnectlink message to the scheduler.

Table I summarizes the scaling primitives used in Chaos. Scale-out causes the most delay due to the need to synchronize training state, while others involve only light communication delays that are negligible. For their implementation details, please go to Section IV-B.

Network Resource Monitoring. When a new node joins, Chaos invokes Algorithms 1 and 2, which rely on propagation delay $t_{u \to v_{\rm new}}^{\rm prop}$, transmission delay $t_{u \to v_{\rm new}}^{\rm trans}$, and synchronization delay $\tau_u^{\rm sync}$. At this point, the cluster monitor activates network resource monitoring. Propagation and transmission delays are measured using iperf, while synchronization delay is measured with timestamps, one recorded before and one after all-reduce. Their difference gives the synchronization delay. Since iperf is costly, Chaos measures network resources only when needed, typically during scale-out and connect-link.

B. Peer Negotiation Protocols

Figure 4 shows how nodes coordinate for the scaling primitives in Table I. In case one, a node joins and then leaves; in case two, one link is added then another is removed.

Scale-out. As shown in Figs. 4a and 4e, once the new node 4 finishes initialization (e.g., preparing training data, building the model, allocating RAM and VRAM), it sends a join request to the scheduler, including its IP and port, and the IDs of intended neighbors (e.g., nodes 1, 2 in case 1). The scheduler then starts the peer negotiation phase. According to the negotiation plan, the scheduler first instructs the neighbors to establish socket connections with the new node. It then triggers the cluster monitor to gather bandwidth and latency data, and runs Algorithms 1 and 2 to generate a state replication plan. Since the topology has changed, the model synchronization policy should also be updated. After all-reduce is completed for the current iteration, the scheduler sends the state replication policy to the new node and its neighbors, and the model synchronization policy to all nodes. According to the replication policy, neighbor 1 sends its training state shard \mathcal{K}_1 to the new node, while neighbor 2 sends shard K_2 . These steps run asynchronously with gradient computation, so their delays can overlap. Once state replication and gradient computation finish, the node proceeds with all-reduce using the new model synchronization policy.

Scale-in. As shown in Figs. 4b and 4e, after node 4 has joined, we now remove it. To exit, node 4 sends a leave

request to the scheduler. With the scheduler's coordination, it disconnects from neighbor nodes 1 and 2. Since the network topology has changed, the scheduler must also update the model synchronization policy accordingly. All nodes then proceed with all-reduce using the new policy. In a node exit, operations such as disconnecting links and updating model synchronization policy happen after all-reduce. But for a node failure, they should be performed before all-reduce to avoid networking errors. If the failure happens during all-reduce, the scheduler notifies all nodes to restart all-reduce. Besides, a node failure is triggered when the scheduler misses heartbeats from node 4 for too long, then the scale-in negotiation will start automatically. The rest follows the same steps as a normal exit.

Connect-link. As shown in Figs. 4c and 4f, we add a new link between nodes 1 and 4. In this case, node 4 sends a link join request to the scheduler, asking to connect to node 1. The scheduler starts peer negotiation and instructs both nodes to establish the socket. Once connected, the cluster monitor gathers network data and updates the model synchronization policy. Since the cluster monitor needs an active socket to measure bandwidth and latency, monitoring should happen after the link is up. While network measurement adds some latency, it overlaps with all-reduce and gradient computation, so its delay can be hidden. After the current all-reduce completes, the scheduler notifies all nodes to update their model synchronization policy and continue with this new setting.

Disconnect-link. As shown in Figs. 4d and 4f, now we remove the link between nodes 2 and 4. In this case, node 4 sends a link leave request to the scheduler, asking to disconnect from node 2. Once the current all-reduce finishes, nodes 2 and 4 disconnect from each other under the scheduler's coordination. Then, each node updates its model synchronization policy to adapt to the new topology. The disconnect-link delay is negligible because it overlaps with gradient computation. If a link fails, e.g., all-reduce or iperf crashes between nodes 2 and 4, node 4 sends a link leave request to the scheduler. The scheduler then instructs all nodes to update the model synchronization policy and restart all-reduce.

C. Overlap Analysis

Chaos achieves the low latency in Table I not only due to its efficient state replication, but also thanks to the overlap between model training and peer negotiation. In Fig. 5a, when a new node joins during all-reduce, the control thread handles socket setup and resource monitoring in parallel. Although resource monitoring incurs some delay, this delay is largely hidden by all-reduce. After that, state replication overlaps with gradient computation, allowing a part of replication delay to be hidden. This overlap further reduces scale-out delay beyond what is achieved by multi-neighbor replication with shard assignment. Another example is shown in Fig. 5b, where connect-link has no state replication, so its delay is fully hidden by gradient computation. Scale-in and disconnect-link are even lighter because they don't require resource monitoring. This explains why scale-in, connect-link, and disconnect-link

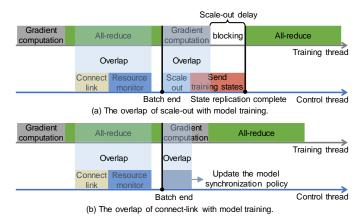


Fig. 5: The overlap between (a) scale-out, (b) connect-link with model training.

consistently stay under 1 millisecond (see Table I and Fig. 9) even in a high-latency edge network.

V. System Design and Integration

In the previous section, we introduced how the scheduler and nodes interact with others, along with the cluster monitor inside the scheduler. This section dives into the internal components of the scheduler and training nodes, detailing their functions and interactions. We then show how to integrate Chaos into DL frameworks such as PyTorch. Unlike other systems [11], [15], [26], Chaos supports flexible all-reduce implementations beyond just parameter server architectures.

A. System Design

Fig. 6 illustrates the overall architecture of Chaos with two main types of nodes: the training nodes and the scheduler.

- 1) Training nodes: Training nodes are the core compute units powered by three components.
 - Communication stack handles data exchange between training nodes, e.g., weights, gradients, and training state.
 - DL framework runs the training pipeline, including data preparation, gradient computation, and parameter updates.
 Common frameworks like PyTorch, TensorFlow, and MXNet can be used here.
 - Agent bridges the node and scheduler. On the northbridge, it monitors local status, detects node and link changes, reports events to the scheduler to trigger actions such as scale-out, scale-in, connect-link, and disconnect-link. It also executes commands from the scheduler, such as connecting to new neighbors, disconnecting links, sending or receiving training states, and updating the local model synchronization policy. On the southbridge, the agent coordinates computation and communication. For example, establishing or closing sockets, updating communication rules (e.g., which data to send or receive), synchronizing training state for new nodes, and handling faults like blocking and restarting all-reduce.

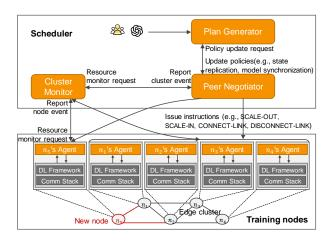


Fig. 6: System overview.

2) Scheduler: The scheduler is Chaos's brain and can be deployed on any node. Its cluster monitor tracks cluster topology, network resources, and scaling events reported by node agents, then passes this data to the peer negotiator to take actions based on the protocols described in Section IV-B. For each event, the scheduler should update the model synchronization policy since the topology has changed, and for scale-out, it also updates the state replication policy. These policies are generated by the plan generator using data from the cluster monitor. Algorithms 1 and 2 outputs the state replication policy, while the model synchronization policy follows the all-reduce scheduler's strategy (e.g., FAPT in NetStorm [25]). The plan generator also supports custom policies, such as user-defined or ChatGPT-generated ones.

B. Use Chaos with Deep Learning Frameworks

We designed easy-to-use APIs to enable popular DL frameworks like PyTorch to use Chaos's self-healing and autoscaling features. These APIs include:

- Trainer: A class that, when instantiated, sends a node join request to the scheduler. Then, following the scaleout workflow, it establishes socket connections with its neighbors and synchronizes the training state.
- check_state_replication: This function runs on existing nodes to check if they need to synchronize training state. If the scheduler issues a replication policy, selected nodes should send their assigned shards to the new node according to the policy.
- capture_exit_event: A helper function that detects if a user node intends to leave. For example, when the user clicks "Quit Cluster" in the GUI or presses "Ctrl+C" in the terminal.
- request_node_exit: Sends a leave request to the scheduler to start the scale-in workflow and safely exit the cluster. It will disconnect from its neighbors.

Listings 1 and 2 show example code for node joining and node leaving. For node joining, on the new node, the user starts

Listing 1: The code example of node joining

```
1
   from chaos.trainer import Trainer
2
3
     Send a join request to the scheduler
   trainer = Trainer()
   # Load data, define model, optimizer, etc.
6
   for batch_data in train_loader:
8
9
     # Forward and backward propagation
10
     # All-reduce and params update
11
12
     trainer.update()
13
     # Pull training states from other nodes
14
15
     trainer.check_state_replication()
```

Listing 2: The code example of node leaving

```
from chaos.trainer import Trainer
   # Init the trainer
3
 4
   trainer = Trainer()
5
6
     Load data, define model, optimizer, etc.
7
   for batch_data in train_loader:
8
       Forward and backward propagation
9
1.0
11
     # All-reduce and params update
     trainer.update()
12
13
       When detecting an exit event, send a
14
         node leave request to the scheduler
15
     if capture_exit_event():
16
       trainer.request_node_exit()
```

the scale-out workflow by creating a Trainer() instance. and other nodes call <code>check_state_replication()</code> after each all-reduce to check if they need to help synchronize the training state to the new node. For node leaving, the node calls <code>capture_exit_event()</code> to check if the user intends to quit. If so, it starts the scale-in workflow by calling <code>request_node_exit()</code>. In these cases, connect-link and disconnect-link are also triggered, since adding a node involves creating new sockets, and node leaving should remove them.

For node and link failures, they require no extra user code. Chaos detects them automatically via heartbeats and probes. Once detected, the scheduler autonomously triggers the corresponding peer negotiation protocol to handle them.

VI. PERFORMANCE EVALUATION

A. Experimental Setup

Testbed setup. We developed the Chaos prototype on ps-lite [27] with 2K LoC and used Docker to virtualize 6-12 nodes. For node changes, new nodes join by randomly connecting to

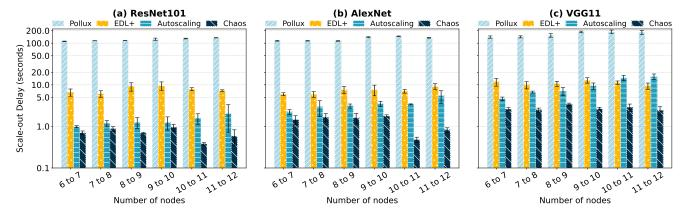


Fig. 7: Comparison of scale-out delays of Pollux, EDL+, Autoscaling, and Chaos.

several running nodes. Nodes exit or failures are triggered by randomly removing a node. For link changes, we randomly connect two nodes to add a link, or disconnect a random link to simulate an exit or a failure. To simulate the dynamic and heterogeneous nature of edge networks, we used Linux tc to randomly set bandwidth between 100-1000 Mbps and update every 3 minutes (as done in [28]–[31]).

Training task. We set up three types of training tasks: (a) Image classification on CIFAR-10 using ResNet101, AlexNet, and VGG11 (ranging from 178 MiB to 528 MiB); (b) Text pre-training on WikiText-2 using GPT-2, GPT-2 medium, and GPT-2 large (ranging from 468 MiB to 3050 MiB); (c) GPT-2 small fine-tuning with LoRA (1.7 MiB) on DailyDialog. The dataset is evenly split to each training node.

Performance metrics. We focus on three metrics: how node joins/leaves affect convergence accuracy, the delay caused by adding/removing nodes and links, and the time wasted waiting.

- Model accuracy: When nodes join or leave, they bring in or take away their training data. The changes in training data can affect both convergence speed and final accuracy.
- Scaling delay: Chaos implements four scaling primitives: scale-in, scale-out, connect-link, and disconnect-link. We measure how long delay each primitive takes.
- Cluster idle time: During scale-out, some nodes pause training for state replication, leaving their GPUs idle. We measure the total GPU idle time across the cluster.

Comparison benchmarks. This section includes a systemwide comparison and two ablation studies. For each, we set the following benchmarks.

- (a) Overall Comparison: To evaluate Chaos's scaling efficiency, we compare it with Pollux, EDL+, and Autoscaling.
 - *Pollux* [8]: Use stop-resume checkpointing to handle scaling, which pauses training and restarts afterwards.
 - *EDL*+: Use stop-free autoscaling with single-source replication. This is an enhanced version of EDL [13], which picks the fastest neighbor for state replication [14], instead of choosing a random node.

- Autoscaling [18]: Use stop-free autoscaling with multisource replication, allowing the new node to pull from multiple nodes in parallel.
- Chaos (ours): Use stop-free autoscaling with multineighbor replication, where the new node pulls from multiple neighbors with smart shard scheduing.
- (b) Ablation Study 1: To evaluate the efficiency of multineighbor replication proposed in Section II-B, we use singlesource replication in EDL+ and multi-source replication in Autoscaling as benchmarks.
 - Single-source replication: The new node pulls the full training state from one fastest neighbor.
 - Multi-source replication: The new node pulls different shards of the training state from several nodes, with even shard scheduling.
 - *Multi-neighbor replication (ours):* The new node pulls different shards of the training state from several neighbors, with even shard scheduling.
- (c) Ablation Study 2: To evaluate the optimality gap of Algorithm 2, we use brute-force search and even assignment as benchmarks.
 - Brute-force search (lower bound): Search all possible assignments in P3 to find the optimal solution.
 - Even shard assignment (upper bound): Assign model shards evenly across nodes.
 - Greedy shard assignment (ours): Use Algorithm 2 to find a near-optimal solution, aiming to match the lower bound.

B. Scale-out Delays of Pollux, EDL+, Autoscaling and Chaos

In this experiment, we compare the scale-out delay of Pollux, EDL+, Autoscaling, and Chaos, as shown in Fig. 7. Each experiment was repeated 4 times. The x-axis labels like "6 to 7" mean one node was added to a 6-node cluster during training, others follow the same pattern.

Different scaling strategies lead to dramatic differences in scale-out delays. Pollux has the highest delay, over 100 seconds, mainly due to checkpointing, which requires writing and reading the training state to and from a slow disk, causing heavy disk I/O overhead. EDL+, Autoscaling, and Chaos avoid disk access and instead use the network to pull the training state, thus achieving much lower delays. However, EDL+ still faces delays above 10 seconds for larger models because it transfers the entire training state from a single node to the new node, creating a bottleneck as model size grows. Autoscaling is faster than EDL+ in small setups, but its performance drops as cluster and model scale up, eventually lagging behind EDL+. The main issue is redundant traffic: since all nodes share identical training states, multi-hop transfers add no value, they just wasted bandwidth. As the model and cluster size grow, this overhead becomes even more pronounced. Chaos, by constrast, pulls the training state from multiple neighbors. This reduces network hops and better utilizes the bandwidth of multiple links on the new node, thus speeding up transmission. In addition, with a smart shard scheduler, Chaos further balances traffic across these parallel links and minimizes the overall replication time. With these optimizations, Chaos cuts scaleout delay to about 1 second.

We also find that Chaos offers superior scalability. As the cluster grows, delays increase for Pollux, EDL+ and Autoscaling, but Chaos's delay stays flat, and even drops when the cluster grows beyond 10 nodes. This is because a larger cluster gives the new node more neighbors and greater parallel bandwidth, thus speeding up state transfer. This advantage is unique to Chaos, EDL+ and Autoscaling cannot achieve it, since bigger networks mean longer transfer paths and more chances for bandwidth bottlenecks. Results on text generation tasks with GPT-2 models confirm this as well. As shown in Fig. 8, as model size grows, scale-out delays increase linearly, but stay stable as the cluster gets larger.

C. Cluster Idle Time of Pollux, EDL+, Autoscaling and Chaos

Cluster idle time is the total idle time of affected nodes during scale-out. It reflects how much computing resources is wasted, and it is different from scale-out delay. A system might have a high scale-out delay but affect only one node, making total idle time low; or have a low scale-out delay but affect all nodes, making total idle time high (e.g., Autoscaling). Fig. 10 compares the cluster idle time across Chaos, Autoscaling, EDL+, and Pollux. Among them, Pollux wastes the most resources, with cluster idle time exceeding 1000 seconds. Its high scale-out delay and cluster restarts block all nodes. Next is EDL+, with idle time between 50 and 100 seconds. Although the new node pulls from only one node, an extra barrier in EDL+ forces all nodes to wait, making the total idle time high. Autoscaling also shows high idle time because all nodes participate in state replication, and its scale-out delay grows quickly as the cluster expands. In contrast, Chaos consistently keeps cluster idle time under 10 seconds. This is thanks to its fast scale-out and efficient design: only a few neighbors handle state replication while the rest continue training. With scalable scale-out delays and a limited number of neighbors, Chaos keeps idle time low and unaffected by cluster size, showing excellent scalability and resource efficiency.

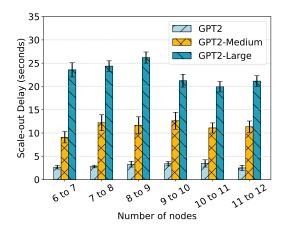


Fig. 8: Scale-out delays of Chaos on GPT-2 models.

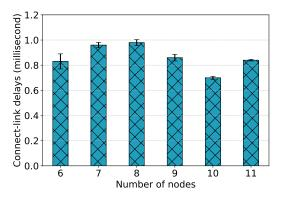


Fig. 9: Connect-link delays of Chaos as cluster size grows.

D. Scale-in and Connect / Disconnect-link Delays of Chaos

In the above, we focused on scale-out because it requires pulling training state from other nodes, leading to noticeable communication delays. In contrast, other primitives, scale-in, connect-link, and disconnect-link, only exchange tiny control messages, and they overlap with costly operations like all-reduce and gradient computation, so their delays are hidden. In this experiment, we keep the number of nodes fixed and use connect-link to add a link between two random nodes. The results are shown in Fig. 9. The connect-link delay remains under 1 millisecond and is unaffected by cluster size. This result also applies to scale-in and disconnect-link. As a result, there is little value in comparing them across systems since they are never a bottleneck and all perform well in practice.

E. How Scale-in/out Affects Convergence?

Adding or removing nodes brings in or takes away training data, so in this experiment, we explore how scale-out and scale-in affect model convergence, including ResNet101, AlexNet, and VGG11. Their accuracy curves are shown in Figs. 11 and 12, respectively. For scale-out, training starts with 4 nodes, and a new node is added at the 100th epoch (green). Before the new node joins, the scale-out curve (green) closely

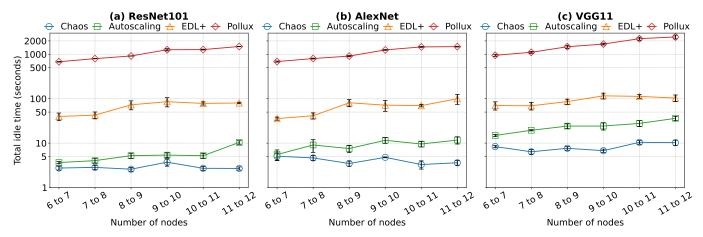


Fig. 10: The total GPU idle time across the cluster during each scale-out.

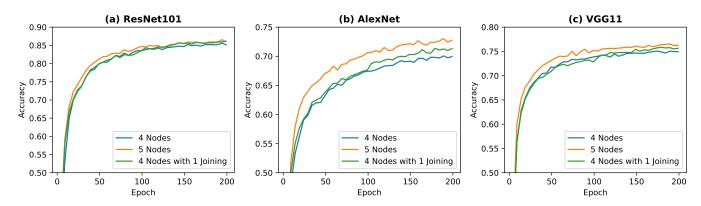


Fig. 11: The effects of scale-out on ResNet101, AlexNet, VGG11 convergence.

tracks the 4-node curve (blue), and it smoothly shifts toward the 5-node curve (orange) after the new node joins. For scale-in, training starts with 5 nodes, and one node is removed at the 100th epoch (green). Before a node leaves, the scale-in curve follows the 5-node curve and gradually shifts toward the 4-node curve afterward. Even after the node leaves, the model retains knowledge from its data. The same pattern was found when fine-tuning GPT-2 with LoRA, as shown in Figs. 13 and 14, but nodes are added or removed at epoch 3. This shows *Chaos also works well for LLM fine-tuning*.

Notably, both scale-out and scale-in curves stay smooth during node changes, with no sharp fluctuations, because deep models are robust to small changes in training data, minor additions or removals do not disrupt convergence. And since we change only one node at a time, the noise is further diluted by global averaging. This feature makes Chaos well-suited for edge DML training and fine-tuning, where nodes are free to join and leave, usually one by one, following a Poisson process, instead of in batches like on the cloud.

F. Ablation Study on State Replication Mechanism

State replication is key to a fast scale-out. In this experiment, we conduct ablation studies on the state replication mechanism

of EDL+, Autoscaling, and Chaos to evaluate how effective our multi-neighbor replication is versus single-source and multi-source replication, and how small the optimality gap is between our greedy shard assignment and the optimum.

The multi-neighbor approach is inherently superior. In this study, the single-source approach picks the fastest neighbor, while multi-source and our multi-neighbor approaches use equal shard splits across nodes. As shown in Fig. 15, the multi-neighbor approach offers much lower scale-out delays than both single- and multi-source approaches, and in most cases, multi-source is even slower than single-source. This matches the analysis in Fig. 1. As discussed in Section II-B, relying on a single source creates bandwidth and load bottlenecks that only get worse as models and clusters scale up. While with multi-source replication, it still suffers from rapidly increasing delays due to redundant traffic and multi-hop forwarding. Multi-neighbor replication improves it by pulling only from neighbors, cutting out redundant traffic and long network paths, making it the standout approach.

Our greedy assignment is empirically near-optimal. By default, multi-neighbor replication assigns equal shard sizes to all neighbors, which we treat as the worst-case upper bound. We use brute-force search to find the global optimum as a

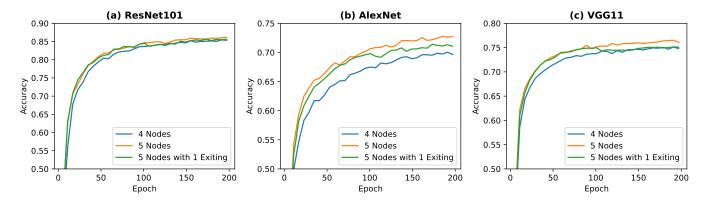


Fig. 12: The effects of scale-in on ResNet101, AlexNet, VGG11 convergence.

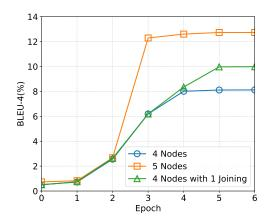


Fig. 13: The effects of scale-out on GPT-2 convergence.

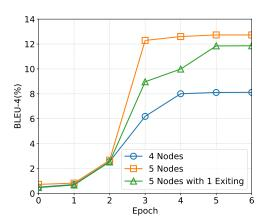


Fig. 14: The effects of scale-in on GPT-2 convergence.

lower bound. The closer we are to this lower bound, the better the shard assignment. As shown in Fig. 16, our greedy assignment stays within 0.5%–29% of the optimal, matching the analysis in Section III-B. This confirms that Algorithm 2 is easy-to-use, fast, and effective, making it a top choice for real-world deployment.

By combining the multi-neighbor replication with a smart

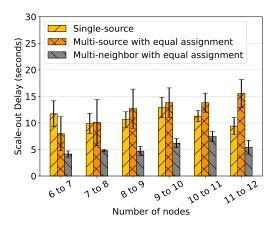


Fig. 15: Comparison of scale-out delays for single-source, multi-source and multi-neighbor replication.

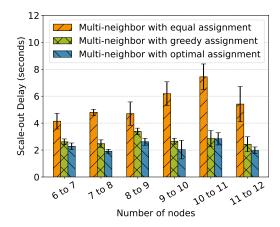


Fig. 16: Comparison of equal, greedy, and optimal assignment for multi-neighbor replication.

shard scheduler, Chaos keeps scale-out delays lower and more stable, and can be even faster as the cluster grows.

VII. CONCLUSION

This paper presents Chaos, a resilient and scalable edge DML training system with built-in self-healing and autoscal-

ing. It implements four primitives: scale-out, scale-in, connect-link, and disconnect-link, to handle node and link joins, exits, and failures. To speed up scale-out, Chaos features multineighbor replication with fast shard scheduling to reduce state replication delay. A built-in cluster monitor tracks resource and topology changes, feeding real-time network data to the scheduler for scaling decisions. Through peer negotiation protocols, Chaos handles scaling events in a self-governed, decentralized manner, but not centrally managed by an admin. Experiments show that Chaos consistently achieves much lower scale-out delays than Pollux, EDL, and Autoscaling, and handles scale-in, connect-link, and disconnect-link events in under 1 millisecond, making it smoother to handle joins, exits, and failures. It also delivers the lowest idle time, showing superior resource use and scalability as the cluster grows.

REFERENCES

- [1] S. Altman, T. Amin, P. Alex, and S. Daniel, "Pre-training gpt-4.5," https://www.youtube.com/watch?v=6nJZopACRuQ, 2025.
- [2] D. AI, "Day 6 one more thing: Deepseek-v3/r1 inference system overview," https://github.com/deepseek-ai/open-infra-index/blob/main/ 202502OpenSourceWeek/day_6_one_more_thing_deepseekV3R1_ inference_system_overview.md, March 2025.
- [3] A. Maurya, R. Underwood, M. M. Rafique, F. Cappello, and B. Nicolae, "Datastates-Ilm: Lazy asynchronous checkpointing for large language models," in *Proceedings of the 33rd International Symposium on High-Performance Parallel and Distributed Computing*, 2024, pp. 227–239.
- [4] T. Gupta, S. Krishnan, R. Kumar, A. Vijeev, B. Gulavani, N. Kwatra, R. Ramjee, and M. Sivathanu, "Just-in-time checkpointing: Low cost error recovery from deep learning training failures," in *Proceedings of* the Nineteenth European Conference on Computer Systems, 2024, pp. 1110–1125.
- [5] A. Eisenman, K. K. Matam, S. Ingram, D. Mudigere, R. Krishnamoorthi, K. Nair, M. Smelyanskiy, and M. Annavaram, "{Check-N-Run}: A checkpointing system for training deep learning recommendation models," in 19th USENIX Symposium on Networked Systems Design and Implementation (NSDI 22), 2022, pp. 929–943.
- [6] I. Jang, Z. Yang, Z. Zhang, X. Jin, and M. Chowdhury, "Oobleck: Resilient distributed training of large models using pipeline templates," in *Proceedings of the 29th Symposium on Operating Systems Principles*, 2023, pp. 382–395.
- [7] T. He, X. Li, Z. Wang, K. Qian, J. Xu, W. Yu, and J. Zhou, "Unicron: Economizing self-healing llm training at scale. arxiv e-prints, article," arXiv preprint arXiv:2401.00134, 2023.
- [8] A. Qiao, S. K. Choe, S. J. Subramanya, W. Neiswanger, Q. Ho, H. Zhang, G. R. Ganger, and E. P. Xing, "Pollux: Co-adaptive cluster scheduling for goodput-optimized deep learning," in 15th {USENIX} Symposium on Operating Systems Design and Implementation ({OSDI} 21), 2021.
- [9] Z. Chen, X. Zhao, C. Zhi, and J. Yin, "Deepboot: Dynamic scheduling system for training and inference deep learning tasks in gpu cluster," *IEEE Trans. Parallel Distrib. Syst.*, vol. 34, no. 9, pp. 2553–2567, 2023.
- [10] W. Xiao, R. Bhardwaj, R. Ramjee, M. Sivathanu, N. Kwatra, Z. Han, P. Patel, X. Peng, H. Zhao, Q. Zhang et al., "Gandiva: Introspective cluster scheduling for deep learning," in 13th USENIX Symposium on Operating Systems Design and Implementation (OSDI 18), 2018, pp. 595–610.
- [11] K. Ma, Z. Cai, X. Yan, Y. Zhang, Z. Liu, Y. Feng, C. Li, W. Lin, and J. Cheng, "Pps: Fair and efficient black-box scheduling for multi-tenant gpu clusters," *Parallel Computing*, vol. 120, p. 103082, 2024.
- [12] X. Zhang, H. Zhao, W. Xiao, X. Jia, F. Xu, Y. Li, W. Lin, and F. Liu, "Rubick: Exploiting job reconfigurability for deep learning cluster scheduling," arXiv preprint arXiv:2408.08586, 2024.
- [13] Y. Wu, K. Ma, X. Yan, Z. Liu, Z. Cai, Y. Huang, J. Cheng, H. Yuan, and F. Yu, "Elastic deep learning in multi-tenant gpu clusters," *IEEE Trans. Parallel Distrib. Syst.*, vol. 33, no. 1, pp. 144–158, 2021.

- [14] L. Xie, J. Zhai, B. Wu, Y. Wang, X. Zhang, P. Sun, and S. Yan, "Elan: Towards generic and efficient elastic training for deep learning," in 2020 IEEE 40th International Conference on Distributed Computing Systems (ICDCS). IEEE, 2020, pp. 78–88.
- [15] S. Wang, A. Pi, and X. Zhou, "Elastic parameter server: Accelerating ml training with scalable resource scheduling," *IEEE Trans. Parallel Distrib. Syst.*, vol. 33, no. 5, pp. 1128–1143, 2021.
- [16] R. Zheng, L. Qu, T. Chen, K. Zheng, Y. Shi, and H. Yin, "Personalized elastic embedding learning for on-device recommendation," *IEEE Transactions on Knowledge and Data Engineering*, vol. 36, no. 7, pp. 3363–3375, 2024.
- [17] Z. Chen, X. Zhao, C. Zhi, and J. Yin, "Deepboot: Dynamic scheduling system for training and inference deep learning tasks in gpu cluster," *IEEE Transactions on Parallel and Distributed Systems*, 2023.
- [18] A. Or, H. Zhang, and M. Freedman, "Resource elasticity in distributed deep learning," *Proceedings of Machine Learning and Systems*, vol. 2, pp. 400–411, 2020.
- [19] J. Mohan, A. Phanishayee, and V. Chidambaram, "{CheckFreq}: Frequent, {Fine-Grained} {DNN} checkpointing," in 19th USENIX Conference on File and Storage Technologies (FAST 21), 2021, pp. 203–216.
- [20] Z. Wang, Z. Jia, S. Zheng, Z. Zhang, X. Fu, T. E. Ng, and Y. Wang, "Gemini: Fast failure recovery in distributed training with in-memory checkpoints," in *Proceedings of the 29th Symposium on Operating* Systems Principles, 2023, pp. 364–381.
- [21] T. Chen, M. Li, Y. Li, M. Lin, N. Wang, M. Wang, T. Xiao, B. Xu, C. Zhang, and Z. Zhang, "Mxnet: A flexible and efficient machine learning library for heterogeneous distributed systems," arXiv preprint arXiv:1512.01274, 2015.
- [22] Y. Ma, D. Yu, T. Wu, and H. Wang, "Paddlepaddle: An open-source deep learning platform from industrial practice," Frontiers of Data and Domputing, vol. 1, no. 1, pp. 105–115, 2019.
- [23] J. Zhou, K. Zhang, F. Zhu, Q. Shi, W. Fang, L. Wang, and Y. Wang, "Elasticdl: A kubernetes-native deep learning framework with fault-tolerance and elastic scheduling," in *Proceedings of the Sixteenth ACM International Conference on Web Search and Data Mining*, 2023, pp. 1148–1151.
- [24] R. L. Graham, "Bounds on multiprocessing timing anomalies," SIAM journal on Applied Mathematics, vol. 17, no. 2, pp. 416–429, 1969.
- [25] Z. Li, W. Feng, W. Cai, H. Yu, L. Luo, G. Sun, H. Du, and D. Niyato, "Accelerating geo-distributed machine learning with network-aware adaptive tree and auxiliary route," *IEEE/ACM Trans. Netw.*, no. 01, pp. 1–16, 2024.
- [26] PaddlePaddle, "Elastic deep learning (edl)," https://github.com/ PaddlePaddle/edl, 2019, online.
- [27] H. Zhou, Z. Li, H. Yu, L. Luo, and G. Sun, "Nbsync: Parallelism of local computing and global synchronization for fast distributed machine learning in wans," *IEEE Trans. Serv. Comput.*, vol. 16, no. 6, pp. 4115– 4127, 2023.
- [28] Y. Wang, S. Yang, X. Ren, P. Zhao, C. Zhao, and X. Yang, "Industedge: A time-sensitive networking enabled edge-cloud collaborative intelligent platform for smart industry," *IEEE Transactions on Industrial Informatics*, vol. 18, no. 4, pp. 2386–2398, 2021.
- [29] P. K. Quan, M. Kundroo, and T. Kim, "Experimental evaluation and analysis of federated learning in edge computing environments," *IEEE Access*, vol. 11, pp. 33 628–33 639, 2023.
- [30] X. Yang, H. Lin, Z. Li, F. Qian, X. Li, Z. He, X. Wu, X. Wang, Y. Liu, Z. Liao et al., "Mobile access bandwidth in practice: Measurement, analysis, and implications," in Proceedings of the ACM SIGCOMM 2022 Conference, 2022, pp. 114–128.
- [31] S. R. Das, S. S. Sarma, M. Khuntia, I. Roy, K. Sinha, and B. P. Sinha, "A novel routing strategy towards achieving ultra-low end-to-end latency in 6g networks," *International Journal of Computer Networks & Communications (IJCNC)*, vol. 14, no. 1, pp. 1–24, 2022.